JOURNAL OF AGRICULTURAL AND FOOD CHEMISTRY

Article

Deconvoluting the dual antiplatelet activity of a plant extract

Vassiliki G. Kontogianni, Maria E. Tsoumani, Tahsin F Kellici, Thomas Mavromoustakos, Ioannis P. Gerothanassis, Alexandros D. Tselepis, and Andreas G. Tzakos

J. Agric. Food Chem., **Just Accepted Manuscript** • DOI: 10.1021/acs.jafc.6b00544 • Publication Date (Web): 10 May 2016

Deconvoluting the dual antiplatelet activity of a plant extract

Vassiliki G. Kontogianni[1#], *Maria E. Tsoumani*[2#], *Tahsin F. Kellici*[1,3], *Thomas Mavromoustakos*[3], *Ioannis P. Gerothanassis*[1], *Alexandros D. Tselepis*[2], *Andreas G. Tzakos*[1,*]

[1]Laboratory of Organic Chemistry, Department of Chemistry, 45110 Ioannina, Greece

[2]Atherothrombosis Research Centre / Laboratory of Biochemistry, Department of Chemistry, 45110 Ioannina, Greece

[3]Laboratory of Organic Chemistry, Department of Chemistry, National and Kapodistrian University of Athens, Athens

# Equal contribution

[*]Corresponding author: Tel: +302651008387, e-mail: agtzakos@gmail.com

Abstract: A thorough evaluation of the antiplatelet activity profile of hexane olive leaf extract in human platelets indicated a potent activity accomplished through a two axis inhibition of platelets activation triggered both by ADP and thrombin. To delineate the extract components responsible for this dual activity an NMR based method was established to determine and quantify the triterpenoid content leading to the characterization of uvaol, erythrodiol and oleanolic acid. The antiplatelet profile of the total extract and of the 3 determined triterpenoids was evaluated against *in vitro* platelet aggregation induced by several platelet agonists as also on PAC-1 binding and P-selectin membrane expression both in healthy volunteers as well in platelets from patients with an acute coronary syndrome receiving dual antiplatelet therapy with aspirin and ticagrelor. The extract was identified to inhibit ADP-induced platelet activation due to its erythrodiol content and TRAP-induced platelet activation due to the activity of uvaol and oleanolic acid.

Keywords: Antiplatelet activity, Cardiovascular disease, Human platelets, Olive leaf extract, Triterpenes

Introduction

The incidence and prevalence of cardiovascular diseases (CVD) have significantly increased in recent years and are driven by genetic and environmental factors (dyslipidemia, hypertension, smoking, diabetes, and obesity)[1]. Platelet aggregation is the primary event in arterial thrombosis at sites of vascular injury. Furthermore, platelets may set an important role in atherogenesis via the secretion or membrane expression of various mediators. Among them, platelet-derived P-selectin may contribute to atherosclerotic lesion development and arterial thrombogenesis through several mechanisms, such as the formation of large stable platelet-leukocyte aggregates [2].

Antiplatelet therapy has been utilized to prevent and treat CVD [3]. However, current antiplatelet therapy is linked with increased bleeding complications, and some antiplatelet drugs (aspirin and clopidogrel) suffer from limited efficacy in some patients due to drug resistance[4]. Thus, there is an immense need for refinement of current antiplatelet treatment and establishment of novel antiplatelet agents with increased efficacy and safety profile. A triple antiplatelet therapy with clopidogrel, aspirin and vorapaxar has been recently established in the secondary prevention of an atherothrombotic event in patients with an acute myocardial infarction and in those with peripheral artery disease [5]. Through this treatment platelet activation pathways mediated via the cyclooxygenase-1 (COX-1), $P2Y_{12}$and protease-activated receptor-1(PAR1) receptors are inhibited. However, due to the combinatorial use of three different drugs side effects, particularly bleeding, could emerge. Plants have traditionally served as a rich reservoir of bioactive compounds [6-13]. A plant extract supplement containing components that bear multifunctional activity and

target multiple receptors mediating platelet activation could be a powerful alternative. Indeed, numerous natural products (alkaloids, polyphenols, fatty acids, and terpenoids, among others) have been marked with an inhibitory activity on platelet's function[14]. Interestingly, some natural compounds from fruit, vegetables and beverages, consumed regularly in the diet may have protective effects in primary and secondary prevention of CVD[15-17]. Natural products that may affect the development of CVD could be compounds derived from olive tree (*Olea europaea* L.)[18].

Olive tree leaves have been widely used in traditional remedies in European and Mediterranean countries. They have been utilized in the human diet as herbal tea, an extract, and powder, and they are consisted of numerous bioactive compounds that may confer a diverse activity profile such as antihypertensive, antioxidant, anti-inflammatory, antiatherogenic, hypoglycemic and hypocholesterolemic[19]. It was demonstrated olive leave polyphenols were able to activate *in vitro* platelets in healthy males possibly via their H_2O_2 scavenging properties. Inhibition of platelet activation has been also linked to a synergistic effect of numerous polyphenols, in contrast to oleuropein alone (the most abundant ingredient)[20]. This finding was in agreement with previous work where 2-(3,4-dihydroxyphenyl)-ethanol (DHPE) components of the phenolic fraction of olive oil can inhibit platelet function and eicosanoid formation *in vitro*[21]. Moreover, it was reported that platelet-activating factor (PAF) antagonists in olive oil exert significant antiatherosclerotic activity in rabbits[22]. Polyphenols have been the major compounds of olive tree products explored for their antiplatelet activity.

Olea europaea leaf extracts contain, oleuropein as the main constituent, tetracyclic and pentacyclic triterpenes, such as erythrodiol, uvaol, and oleanolic acid, sterols. During the

industrial process of extraction, cooling of the hexane solution induce the precipitation of a solid containing triterpenes, fatty acids, flavonoids, saponins, etc. Triterpenes represented 58.1% of the crude extract (the above precipitate), in which erythrodiol, uvaol and oleanolic acid accounted for 27.3, 18.3 and 12.4%, respectively[23].

The current aim was to exploit the triterpenoid profile of an olive leaf hexane extract rich in triterpenoids and free in polyphenols as also to evaluate the antiplatelet profile and the antiplatelet activity of the extract and its major determined triterpenoids. To complement and delineate our experimental findings on a dual antiplatelet activity of the extract an *in silico* study was employed. For the rapid identification and quantification of triterpenoids in crude olive leaf extract, without any former separation step, a strategy based on ^{1}H-^{13}C heteronuclear single-quantum coherence (HSQC) and ^{1}H-^{13}C heteronuclear multiple-bond correlation (HMBC) NMR experiments was employed.

Materials and methods

Solvents and Standards. Oleanolic acid (97%) and uvaol (95%) were purchased from Sigma-Aldrich (Steinheim, Germany) and erythrodiol (>97%) was from Fluka (Steinheim, Germany). Pyridine-d_5 was from Aldrich (Steinheim, Germany), 3-trimethlsilyl-3, 3, 2, 2-tetradeuteriopropionic acid sodium salt (d_4-TMSP) was obtained from Cambridge Isotope Laboratories Inc. (Cambridge, MA). Hexane and methanol were purchased from Scharlau (Barcelona, Spain) ethyl acetate was from Lab-Scan (Dublin, Ireland). Hydroxypropyl-γ-cyclodextrin (HP-γ-CD) was obtained from Aldrich (Steinheim, Germany). HPLC grade acetonitrile was from Scharlau (Barcelona, Spain) and water from ACROS ORGANICS. Potassium dihydrogen phosphate (Pro Analysis) was from Merck (Darmstadt, Germany)

and ortho-phosphoric acid 85% was from Riedel-de Haen (Seelze, Germany).Adenosine diphosphate (ADP) was obtained from Chrono-Log Corp (Havertown, PA, USA). Arachidonic acid (AA) was from Sigma Aldrich, St Louis, MO USA and Thrombin Receptor Activator Peptide-14 (TRAP) was from Bachem, Bubendorf, Switzerland. Fluorescently-labeled monoclonal antibodies, PAC-1-FITC, anti-CD62P-PE and anti-CD61-PerCP were purchased from Beckton Dickinson (San Jose, CA, USA).

Plant Material. Olive leaves were collected from olive trees grown in Northern Greece, as also a sample was obtained from the biological cultivator Maria Komini. Reference specimens are retained in the herbarium of the University of Ioannina with voucher accession number UOI051108.

Extract preparation. The plant material was dried with liquid nitrogen and pulverized into a fine powder. 20.2 g plant was used in the extraction procedure. The leaves were subsequently extracted with hexane (extraction volume 200 ml), and ethyl acetate (extraction volume 200 ml), in a Soxhlet apparatus for ~6 h. The two extracts (hexane and ethyl acetate) were concentrated in a rotary evaporator and kept into sealed flasks.

Instrumentation

NMR experiments. NMR experiments were recorded on a Bruker AV-500 spectrometer. Spectra were obtained from the hexane olive leaf extract dissolved in pyridine-d_5(20 mg of dry material in 0.5 mL of solution in pyridine-d_5). The procedure followed was our method[24], and described in detail in Supporting information (Section S1). All measurements were conducted in triplicate (on three different extracts of the same sample).

HPLC experiments. Instrumentation and methods are described in Supporting information (Section S2). For the analysis of triterpenoids the olive leaf extract was dissolved in methanol (1 mg/mL). The characterization of triterpenoids was based on retention time, UV spectra and spiking. All measurements were performed in triplicate (on three different extracts of the same sample).

Principal Components Analysis. Eleven representative antiplatelet drugs (ticlopidine, clopidogrel, prasugrel, ticagrelor, cangrelor, eptifibatide, dipyridamole, cilostazol, vorapaxar, atopaxar, triflusal and acetyl salicylic acid) were selected for the PCA analysis. The 3D structures of all the drugs and the three natural products (erythrodiol, uvaol and oleanolic acid) were minimized using LigPrep 3.4 [25]and the OPLS2005 force field [26] and they were optimized using a PM3 semiempirical quantum calculation. The topological and physicochemical descriptors were calculated using Canvas 1.5, while descriptors that predict the absorption, distribution, metabolism and excretion of the compounds were calculated using QikProp 4.4 [27]. Eight properties were selected for this analysis: polar surface area (PSA), hydrogen bond acceptors (HBA), hydrogen bond donors (HBD), molecular weight (MW), predicted octanol/water partition coefficient ($\log P_0/w$), conformation-independent predicted aqueous solubility (logS), and the total solvent accessible surface are divided in its hydrophobic (FOSA) and hydrophilic (FISA) components. The Principal Components Analysis was performed using the cheminformatics package Canvas 2.4 [28, 29].

Structure alignment. In order to find potential common features of the antithrombotic drugs with the natural products all the compounds were aligned using Phase 4.3[30]. Conformations for each molecule were generated using ConfGen and by applying the

thorough setting [31]. Phase 4.3 first creates pharmacophoric sites from active compounds. A common pharmacophore is created, grouping similar pharmacophore hypotheses according to the distance between the pharmacophore features. At least 4 pharmacophore features were selected as required match with the active compounds. The created hypotheses are scored and ranked while the quality for each hypothesis is assessed using a survival score.

Induced Fit Docking. The crystal structure of PAR1 (PDB ID code: 3VW7[32]) was prepared using the standard options of the Protein Preparation Wizard [33] (Schrödinger Suite 2015.2). The ligands were built in Maestro 10.2 [34] and were then ionized and minimized using the LigPrep 3.4 software [25] and the OPLS3 force field [35]. The receptor grid was selected with centroid the vorapaxar (the cocrystallized ligand). The ligands were initially docked using Glide 6.7. The receptor van der Waals scaling was set to 0.8. Residues within 5 Å of the ligand pose were refined using Prime 4.0 [36]. The ligands were redocked using the Glide XP algorithm [37].

Prime-MMGBSA: The MM-GBSA method was used to predict the binding energies of erythrodiol, uvaol and olenaolic acid in the PAR-1 crystal structure (PDB ID 3VW7). The resulting poses from the IFD calculations were used as input structures in the Prime software [38]. The binding energy of the complex is then calculated using the equation (1).

$$\Delta G_{\text{binding}} = E\text{complex} - (E_{\text{receptor}} + E_{\text{ligand}}) \quad (1)$$

E_{complex} is the energy of the minimized structure of the complex, E_{receptor} is the energy of the minimized structure of the receptor and E_{ligand} is the energy of the minimized structure

of the ligand. For the calculations the VSGB 2.0 solvation method[39] was used, with the OPLS3 force field [40].

Biological assays. The antiplatelet activity of the total olive leaf extract as well as its main triterpenoids (erythrodiol, uvaol and oleanolic acid), dissolved in DMSO, was studied in platelet-rich plasma (PRP) by using platelet aggregometry and flow cytometry techniques. The final DMSO concentration in each assay was <0.5% (v/v).

Platelet aggregation in PRP of healthy volunteers. Platelet aggregation studies in PRP prepared from peripheral venous blood of apparently healthy volunteers were performed as we previously described[41]. Briefly, the platelet count of PRP was adjusted to a final platelet concentration of 2.5 x 10^8/mL with homologous platelet-poor plasma (PPP). The PRP was then preincubated with total leaf extract as well as with each of the above triterpenoids for 1 min before the initiation of aggregation. Platelet aggregation in the presence of ADP (10 μM), AA (500 μM) and TRAP (10 μM) was determined in aliquots of 0.5mL PRP, in a ChronologLumi-Aggregometer (Model 700 4-Channel) at 37^{o}C, with continuous stirring at 1,200 rpm. 4min after the addition of each agonist, the maximal aggregation was achieved and it was determined and expressed as a percentage of 100% light transmission calibrated for each specimen (maximal percentage of aggregation). The inhibitory efficacy was expressed as IC_{50} values (concentration that induces 50% inhibition of platelet aggregation). All aggregation studies were conducted within 3 h after blood was withdrawn.

Membrane expression of the integrin receptor $\alpha_{IIb}\beta_3$ and P-selectin. The degree of platelet inhibition by the above compounds was also explored by flow cytometry through determination of the membrane expression of the integrin receptor $\alpha_{IIb}\beta_3$ (PAC-1 binding)

and P-selectin with saturating concentrations of PAC-1-FITC and CD62P-PE, respectively. Briefly, platelets in PRP prepared from peripheral venous blood of apparently healthy volunteers were incubated in the presence or in the absence of the compounds. Activation with agonists was performed for 5 min at 37^{o}C without stirring. Platelets were incubated with CD62P-PE and PAC-1-FITC for 20 min in the dark; diluted (1:5, v/v) with 10mM PBS, pH 7.4 and analyzed immediately by flow cytometry (FACsCalibur, Becton-Dickinson, San Jose, CA, USA). Platelets were gated according to staining for the platelet specific antigen, CD61-PerCP. The gated events were further analyzed in histograms using the mean fluorescence intensity (MFI). Flow cytometry results are presented as the MFI of the activated sample minus the MFI of the unactivated sample, as we have previously described[42].

Platelet aggregation in PRP of patients receiving dual antiplatelet therapy.In some experiments (n=5) we prepared PRP from blood of patients with an acute coronary syndrome (ACS) receiving dual antiplatelet therapy with the COX-1 inhibitor aspirin (100mg/day) and ticagrelor (an antagonist of the ADP receptor $P2Y_{12}$) (90 mg x 2/day). The antiplatelet effect of the total olive leaf extract as well as erythrodiol, uvaol and oleanolic acid was studied as above.

The Ethics Committee of the University Hospital of Ioannina approved the study and all participants signed an informed consent form.

Statistical analysis. Results are expressed as mean ± SD. Mean values were compared by Student's t-test with significance defined at a value of $P<0.05$.

Results and discussion

Establishment of an NMR method for the rapid identification and quantitative analysis of triterpenoids in the crude olive leaf extract, without any previous separation step

The hexane extract obtained from olive leaves has been ascribed to contain wax, fatty acids, triterpenes, saponins e.t.c according to literature, with triterpenes representing a significant proportion of the crude extract [23]. In order to exploit the effects of an hexane olive leaf extract on platelet aggregation, it was of importance to determine and quantify the triterpenoids composition on the extract. Based on our former work for the quantitative estimation of triterpenoids[24], we applied and expanded this methodology to the characterization of oleanolic acid, erythrodiol and uvaol in the hexane olive leaf extract. Due to the weak chromophores of these analytes and the concurrent low UV absorption, their resolution by LC is rather difficult. We therefore, employed a strategy based on 2D $^{1}H–^{13}C$ HSQC ($^{1}H–^{13}C$ Heteronuclear Single-Quantum Coherence) and $^{1}H–^{13}C$ HMBC ($^{1}H–^{13}C$ Heteronuclear Multiple-Bond Correlation) NMR experiments. We first recorded ^{1}H-^{13}C HSQC and ^{1}H-^{13}C HMBC spectra of a mixture of oleanolic acid, erythrodiol and uvaol to explore whether their unambiguous identification in the 2D map is feasible.

As illustrated in Figure S1A, the majority of the one-bond proton and carbon nuclei interactions of erythrodiol, oleanolic acid and uvaol are overlapped. However, significant differences exists in a number of cross peaks for each compound given in Table S1. The long range connectivities which are of diagnostic importance for each compound are given in Table S1. These distinct “columns” of cross peaks can allow the identification of

223 oleanolic acid, erythrodiol and uvaol. ^{1}H-^{13}C HSQC and ^{1}H-^{13}C HMBC spectra of the
224 hexane olive leaf extract are illustrated in Figure 1A and 1B, respectively.
225 The diagnostic "columns" of cross peaks for oleanolic acid, erythrodiol and uvaol in the
226 HMBC map and the cross peaks in the HSQC map can be easily identified, allowing the
227 unequivocal assignment of the resonances of these triterpenoids. Thus, the combination of
228 the data extracted through ^{1}H-^{13}C HSQC and ^{1}H-^{13}C HMBC spectral assignment can be
229 used as a sufficient novel analytical tool for the identification of erythrodiol, uvaol and
230 oleanolic acid. The ^{1}H and ^{13}C NMR signals used for quantification and identification of
231 the three molecules (the selected cross peaks plotted as a function of concentration) are
232 reported in Table S1. The peak intensities were estimated as the mean value of the absolute
233 intensities of the cross peaks of C28 to H28a,b and C12 to H12 of erythrodiol and uvaol
234 and C12–H12 and C18–H18 for oleanolic acid. Linear responses were observed over the
235 range of 4.5 – 13.6 mM for erythrodiol and uvaol. From 2D ^{1}H-^{13}C data acquisitions of 14
236 min could be obtained quantitative results. The concentration limit was found to be 3 mM.
237 The contents of oleanolic acid, erythrodiol and uvaol in the hexane olive leaf extract as
238 determined from 2D NMR measurements were found 56.6±2.5, 67.6±5.2 and 37.8±4.1 mg
239 g^{-1}, respectively.
240 To make a comparison of our NMR data, detailed HPLC measurements were also carried
241 out. For the HPLC analysis of erythrodiol and uvaol the inclusion of derivatized
242 cyclodextrins (DM-β-CD, HP-γ-CD) to the acetonitrile-phosphate buffer mobile phase was
243 utilized to enhance the resolution [43]. The use of cyclodextrins for the simultaneous
244 determination of erythrodiol and uvaol is reported for the first time herein. Using a flow
245 rate 1.0 mL min^{-1}, the retention times for oleanolic acid, uvaol and erythrodiol were 27.0,

46.0 and 48.7 min, respectively, as shown in Figure 2A. The respective HPLC concentration levels for oleanolic acid, erythrodiol and uvaol in the hexane olive leaf extract that were found to be 58.4 ± 1.8, 58.5 ±5.8 and 40.9 ± 3.7 mg g^{-1} are in good agreement with the 2D NMR measurements.

Effect of total leaf extract and its main triterpenoids on platelet aggregation in healthy volunteers

Three platelet activation pathways are considered particularly important in the development of atherothrombosis and are triggered by ADP via the $P2Y_{12}$ receptor, thrombin via the PAR1 and COX-1 mediated thromboxane A_2 (TxA_2) synthesis and subsequent platelet activation via the TxA_2 receptor.

As shown in Table 1, the total leaf extract is potent in inhibiting platelet aggregation induced by ADP or TRAP. This effect was dose-dependent and the IC_{50} values were 512 μg/ml for ADP and 320 μg/ml for TRAP. By contrast, no inhibitory effect was observed when AA was used as an agonist. Typical aggregation curves illustrating the dose-dependent inhibitory effect of total leaf extract in TRAP-induced platelet aggregation are presented in Figure 2B.

The effect of the three different terpenoids on platelet aggregation induced by the above agonists resulted in different inhibitory profile (Table 1). Specifically, erythrodiol inhibited ADP-induced platelet aggregation in a dose-dependent manner with an IC_{50} value of 205 μM. The maximum inhibition of 42 ± 3% was observed at the concentration of 410 μM (Table 1). By contrast, erythrodiol did not affect TRAP- and AA-induced platelet aggregation. Uvaol exhibited a great, dose-dependent inhibitory effect on TRAP-induced platelet aggregationwith an IC_{50} value of 100μM. The maximum inhibition of 98.5±1.5%

was evident at the concentration of 300 μM (Table 1). Uvaol exhibited a low inhibitory effect when AA was used as an agonist (32.0 ± 8.0%), whereas no inhibition was observed when we activated platelets with ADP. Finally, oleanolic acid significantly inhibited platelet aggregation induced by TRAP in a dose-dependent manner with an IC_{50} value of 140 μM. The maximum inhibition of 56.7±3.9% was observed at the concentration of 210 μM (Table 1). Oleanolic acid did not affect platelet aggregation induced by ADP and AA. Previous studies have provided contradictory results concerning the effect of oleanolic acid on aggregation of platelets prepared from various animal species. Some studies had shown enhancement of ADP-induced platelet aggregation [44, 45] whereas other studies showed an inhibitory effect[46]. To the best of our knowledge, this is the first study performed in human platelets showing inhibitory effect of the oleanolic acid. The above differences could be possibly attributed to structural differences of platelet's receptors among the various species.

Effect of total extract of olive leaves and its main triterpenoids on $\alpha_{IIb}\beta_3$and P-selectin membrane expression

The above results prompted us to further explore not only platelet aggregation but also platelet secretion. Platelet secretion of bioactive mediators during exocytosis delivers many proteins into the circulation while this process also changes the composition of the platelet membrane, resulting in surface expression of P-selectin and an enhancement in the number of integrin-receptor $\alpha_{IIb}\beta_3$molecules [47]. The exposure of P-selectin is crucial for recruitment of leukocytes to sites of vascular injury and the formation of leukocyte-platelet aggregates, while it is also important for platelet interaction with the endothelium as well as with progenitor endothelial cells [36]. The integrin-receptor $\alpha_{IIb}\beta_3$ in its activation state

292 mediates platelet aggregation by binding fibrinogen [48]. It is also important for further
293 platelet activation through an outside-in signaling pathway [49]. Here, we measured the
294 possible inhibitory effect of a hexane olive leaves extract and its compounds on the P-
295 selectin and $\alpha_{IIb}\beta_3$expression (PAC-1 binding) induced by various platelet agonists.
296 Total olive leaf extract showed great inhibitory effect in PAC-1 binding when we activated
297 platelets with ADP and TRAP (67.5 ± 8% and 65.5 ± 5 %, respectively). On the other
298 hand, total olive leaf extract inhibited P-selectin expression when platelets were activated
299 with TRAP (49.6 ± 8%) whereas it showed no significant inhibitory effect when platelets
300 were activated with ADP (12.0 ± 6 %) (Table 1).
301 Erythrodiol, uvaol and oleanolic acid differentially affected platelet activation induced by
302 ADP and TRAP (Table 1). Erythrodiol at a concentration of 410 μM inhibited PAC-1
303 binding (22± 8%) and P-selectin expression (31± 5%) only when ADP was used as the
304 agonist. Uvaol at a concentration of 300 μM significantly inhibited PAC-1 binding and P-
305 selectin expression induced only by TRAP (85.5±5.2% and 54.8±3.1%, respectively).
306 Similarly, oleanolic acid at a concentration of 210 μM significantly inhibited PAC-1
307 binding and P-selectin expression induced by TRAP (92.0±3% and 75.8±3.4%,
308 respectively.
309 Overall, the above results demonstrate that the total extract of olive leaves inhibit platelet
310 activation induced by ADP and TRAP. Interestingly, its main triterpenoids differentially
311 affect platelet activation, since erythrodiol inhibits only ADP-induced platelet aggregation
312 and secretion (through the $P2Y_{12}$ receptor) whereas uvaol and oleanolic acid primarily
313 inhibit platelet aggregation and secretion induced by TRAP, an agonist of the PAR1 which
314 is the main thrombin receptor on platelets [50].

Effect of total extract of olive leaves and its main triterpenoids on platelets from patients with an acute coronary syndrome receiving dual antiplatelet therapy

The above results suggest that eryhthrodiol, uvaol and oleanolic acid differentially affect platelet activation induced by ADP, AA and TRAP. In order to further establish the differential effect of the main triterpenoids of total olive leaf extract, we further exploited the effect of these compounds on platelet aggregation in PRP prepared from blood of patients with an ACS receiving dual antiplatelet therapy with aspirin and ticagrelor. Through this treatment, two key-pathways (COX-1 andtheP2Y_{12} receptor of ADP) of platelet activation are blocked. However, platelets can still be activated by thrombin via the PAR1. As shown in Figure 3, platelet aggregation to ADP was low due to the inhibitoty effect of ticagrelor, whereas an adequate platelet response to TRAP was observed. It should be stated that the platelet response to AA was very low due to aspirin thus the residual platelet aggregation did not allow us to study the effect of our compounds on AA-induced platelet aggregation. By contrast, the residual aggregatory response to ADP was adequate to permit us to perform our experiments. The total olive leaf extract inhibited both TRAP- and ADP-induced platelet aggregation by 33±2% and 40±3%, respectively (Figure 3). Importantly, triterpenoids differentially affected the platelet aggregation to TRAP and ADP (Figure 3). Specifically, erythrodiol further reduced but not completely abolished residual platelet aggregation induced by ADP in the presence of ticagrelor whereas it did not affect TRAP-induced platelet aggregation (Figure 3). Uvaol and oleanolic acid had no inhibitory effect when platelets were activated with ADP, whereas both compounds inhibited platelet aggregatory response to TRAP by 35.7±4.2% and 33.3±2.8%, respectively (Figure 3).These data further support the results observed in

platelets from healthy volunteers showing the erythrodiol's specificity towards the $P2Y_{12}$ ADP receptor and that of uvaol and oleanolic acid towards PAR1 receptor.

There are few reports in the literature concerning the effect of several members of the triterpenoid family (especially lupane-type triterpenoids, like oleanolic acid) on platelet activation. Regarding the three triterpenoids identified and quantified in the hexane olive leaf extract (oleanolic acid, erythrodiol and uvaol), to the best of our knowledge, this is the first time that the antiplatelet activity of erythrodiol and uvaol is studied.

PCA analysis of terpenoids and antiplatelet drugs

We have first asked the question if the representative drugs, covering various mechanisms of exerting antithrombotic activity, share physicochemical similarities. Predictably, the PCA highlights that the three natural compounds are clustered very closely in the same region of the plot. Furthermore in the same region, very close to the three compounds, are the two drugs vorapaxar and atopaxar (Figure 4.A).

Maps of the physicochemical space sampled by the three natural products and approved antiplatelet drugs, belonging to different families, were created from physicochemical property spaces and visualized by principal component analysis (PCA). In this analysis 11 approved antiplatelet drugs were used that act via inhibiting the $P2Y_{12}$ receptor of ADP, phosphodiesterase, COX-1, PAR1, and integrin receptor $\alpha_{IIb}\beta_3$. The property space was built upon the utilization of 8 calculated structural and physicochemical parameters (polar surface area (PSA), hydrogen bond donors, hydrogen bond acceptors, molecular weight, predicted octanol/water partition coefficient, conformation-independent predicted aqueous solubility and the total solvent accessible surface area). PCA was used to replot the data in a 2-dimensional format (Figure 4A), where the two unitless, orthogonal axes represent

linear combinations of the original 8 parameters. Interestingly, uvaol, oleanolic acid and erythrodiol cluster in one region of the plot that overlaps to the property space sampled by the PAR1 inhibitors vorapaxar and atopaxar (Figure 4A). This result conforms nicely, for uvaol and oleanolic acid, with the experimental results pinpointing that these compounds exert their antiplatelet activity through PAR1.

Pharmacophore alignment of terpenoids and PAR1 inhibitors

The determined similarity, through physico-chemical descriptor metrics, of uvaol and oleanolic acid with vorapaxar and atopaxar, motivated us to explore the existence of probable common pharmacophores in the 3D space. The chemical property space was further investigated by creating common pharmacophore hypotheses. This pharmacophore analysis marked the 3D orientation of chemotypes necessary to binding to PAR1 receptor and to express their inhibitory profile activity in platelet aggregation. The best scoring pharmacophore showed that the natural compounds, vorapaxar and atopaxar share four common features: three hydrophobic interactions and one hydrogen bond acceptor (Figure 4B). All hydrophobic interactions are positioned across the pentacyclic ring system of the natural products. The hydrogen bond acceptor is positioned in the hydroxyl group while in vorapaxar and atopaxar these interactions are positioned in the long hydrophobic spacer. The fact that uvaol, oleanolic acid and erythrodiol share very similar chemical features is reflected on the PCA and pharmacophore analysis where a clear discrimination could not be achieved.

Induced Fit Docking of terpenoids and PAR1 inhibitors in the PAR1 binding site

PCA and pharmacophore alignment correctly predicted the antiplatelet activity of the 3 triterpenoids. However, the different antiplatelet profile of uvaol and oleanolic acid with

respect to erythrodiol, which inhibits platelet aggregation induced by ADP but not TRAP, was not evident through this analysis. This was due to the high similarity of physicochemical features shared by the three natural products and the drugs vorapaxar and atopaxar. To rationalize the differential activity profile of uvaol and oleanolic acid, which we found to act via the PAR1 receptor, with respect to erythrodiol we took advantage of the recently determined X-ray structure of vorapaxar bound to the PAR1 receptor [32]. Through docking calculations of the three triterpenoids to PAR1 we found that oleanolic acid and uvaol share similar docking positions with vorapaxar in contrast to erythrodiol suggesting a possible hypothesis for the different recorded activity.

The critical interactions of vorapaxar involve hydrogen bonds with Leu258, Ala349, Tyr337, π-π interactions with Tyr183 and hydrophobic interactions with Leu262, Leu237, Leu263, Phe271, Ala348, Ala352 and Tyr187 (Figure 5D). The docking positions and key amino acids in the cases of oleanolic acid and uvaol are very similar. Both compounds develop hydrogen bonds with Gly233, Leu237 and Tyr337. Other contacts shared by the two compounds are the hydrophobic contacts with residues Leu333, Tyr353, Val257, Phe271, Pro236, Tyr187 (Figure 5A,B). On the other part, the most favored docking pose of erythrodiol shows hydrogen bonds with Ser344, Tyr350 and Tyr183 (Figure 5C). These differences suggest that, although uvaol and erythrodiol are very similar, their structural differences could induce different favorable poses and could rationalize their different action on the PAR1 receptor. Furthermore calculations using Prime-MMGBSA showed that uvaol and oleanolic acid have similar binding energies (-37.5 and -40.52 kcal/mol correspondingly) (Table 2). The most contributing energetic factors for the two molecules are the lipophilic and Van der Waals (vdW) interactions. The binding energy of the

complex oleanolic:PAR1 is more favored than that of the complex uvaol:PAR1 partially due to adaptation of more negative values of lipophilic and vdW interactions. Erythrodiol, does not have a favoured binding energy (-24.04 kcal/mol) in respect to uvaol and oleanolic acid partially due to adopting less negative values of lipophilic and vdW interactions.

Constructively, in this work a thorough evaluation of the antiplatelet activity profile of a hexane olive leaf extract in human platelets indicated a potent activity accomplished through a two axis inhibition of platelets activation triggered both by ADP and thrombin (TRAP). To delineate the extract components responsible for this dual activity an NMR based method was established to determine and quantify the triterpenoid content, in the crude olive leaf extract, without any previous separation step. The impingement of the three triterpenoids on the three different platelet activation pathways was scrutinized both on platelets from healthy volunteers as well in platelets from patients with an acute coronary syndrome receiving dual antiplatelet therapy. The antiplatelet activity of the extract was not only assigned to the 3 triterpenoids but the dual activity was also deconvoluted to the individual phytochemical components. Specifically, we found that uvaol and oleanolicacid were mainly responsible for the inhibition of the TRAP-induced platelet activation whereas erythrodiol was responsible for the inhibition of the ADP-induced platelet activation. This mapped compound dual activity in a single extract is of importance, since on the basis of a plethora of large-scale clinical trials, the recent guidelines of European Society of Cardiology and the American Heart Association, recommend that ACS patients should be treated with dual antiplatelet therapy including aspirin and an ADP-receptor antagonist (ticagrelor, prasugrel or clopidogrel) [51, 52].

Furthermore, recently FDA approved the use of the specific PAR1 antagonist vorapaxar on top of dual antiplatelet therapy with aspirin and clopidogrel in the secondary prevention of an atherothrombotic event in patients with an acute myocardial infarction and in those with peripheral artery disease [53]. On the basis of our results, the total leaf extract in combination only with aspirin could mimic the antiplatelet effects of the triple antiplatelet therapy (aspirin, ADP antagonist and PAR1 antagonist). Thus, a supplement containing our extract along with aspirin could be useful in the secondary prevention of an atherothrombotic event of patients with an acute myocardial infarction or with peripheral artery disease. The clinical use of this extract could be advantageous over the triple antiplatelet therapy used in the TRA 2P-TIMI 50 (Thrombin-Receptor Antagonist in Secondary Prevention of Atherothrombotic Ischemic Events) trial demonstrating an increased hemorrhagic complication especially for moderate or severe bleeding, including intracranial hemorrhage but not fatal bleeding. A total leaf extract which has the advantage of inhibiting PAR1 receptor in a milder way, could improve the safety profile. However, further studies should be performed to support the above suggestion.

Acknowledgement

This research project has been co-financed by the European Union (European Regional Development Fund- ERDF) and Greek national funds through the Operational Program "THESSALY- MAINLAND GREECE AND EPIRUS-2007-2013" of the National Strategic Reference Framework (NSRF 2007-2013).

Supporting Information

Further information on the NMR and HPLC experiments as well as the ^{1}H-^{13}C HSQC spectrum of the mixture of oleanolic acid, erythrodiol and uvaol and the ^{1}H- NMR

453 spectrum of the mixture of oleanolic acid, erythrodiol and uvaol are available in the
454 Supporting Information.

455 **References**

456 1. Reddy, K. S.; Yusuf, S. Emerging epidemic of cardiovascular disease in
457 developing countries. *Circulation* **1998,** *97*, 596-601.

458 2. Burger, P. C.; Wagner, D. D. Platelet P-selectin facilitates atherosclerotic lesion
459 development. *Blood* **2003,** *101*, 2661-2666.

460 3. Palomo, I.; Toro, C.; Alarcon, M. The role of platelets in the pathophysiology of
461 atherosclerosis (Review). *Mol. Med. Rep.* **2008,** *1*, 179-184.

462 4. Barrett, N. E.; Holbrook, L.; Jones, S.; Kaiser, W. J.; Moraes, L. A.; Rana, R.;
463 Sage, T.; Stanley, R. G.; Tucker, K. L.; Wright, B.; Gibbins, J. M. Future innovations in
464 anti-platelet therapies. *Br. J. Pharmacol.* **2008,** *154*, 918-939.

465 5. Bonaca, M. P.; Scirica, B. M.; Creager, M. A.; Olin, J.; Bounameaux, H.; Dellborg,
466 M.; Lamp, J. M.; Murphy, S. A.; Braunwald, E.; Morrow, D. A. Vorapaxar in patients
467 with peripheral artery disease: results from TRA2{degrees}P-TIMI 50. *Circulation* **2013,**
468 *127*, 1522-1529, 1529e1521-1526.

469 6. Ferlemi, A. V.; Katsikoudi, A.; Kontogianni, V. G.; Kellici, T. F.; Iatrou, G.;
470 Lamari, F. N.; Tzakos, A. G.; Margarity, M. Rosemary tea consumption results to
471 anxiolytic- and anti-depressant-like behavior of adult male mice and inhibits all cerebral
472 area and liver cholinesterase activity; phytochemical investigation and in silico studies.
473 *Chem. Biol. Interact.* **2015,** *237*, 47-57.

474 7. Vujicic, M.; Nikolic, I.; Kontogianni, V. G.; Saksida, T.; Charisiadis, P.;
475 Orescanin-Dusic, Z.; Blagojevic, D.; Stosic-Grujicic, S.; Tzakos, A. G.; Stojanovic, I.
476 Methanolic extract of Origanum vulgare ameliorates type 1 diabetes through antioxidant,
477 anti-inflammatory and anti-apoptotic activity. *Br. J. Nutr.* **2015,** *113*, 770-782.

478 8. Primikyri, A.; Chatziathanasiadou, M. V.; Karali, E.; Kostaras, E.; Mantzaris, M.
479 D.; Hatzimichael, E.; Shin, J. S.; Chi, S. W.; Briasoulis, E.; Kolettas, E.; Gerothanassis, I.
480 P.; Tzakos, A. G. Direct binding of Bcl-2 family proteins by quercetin triggers its pro-
481 apoptotic activity. *ACS Chem. Biol.* **2014,** *9*, 2737-2741.

482 9. Kellici, T. F.; Ntountaniotis, D.; Leonis, G.; Chatziathanasiadou, M.;
483 Chatzikonstantinou, A. V.; Becker-Baldus, J.; Glaubitz, C.; Tzakos, A. G.; Viras, K.;
484 Chatzigeorgiou, P.; Tzimas, S.; Kefala, E.; Valsami, G.; Archontaki, H.; Papadopoulos, M.
485 G.; Mavromoustakos, T. Investigation of the interactions of silibinin with 2-
486 hydroxypropyl-beta-cyclodextrin through biophysical techniques and computational
487 methods. *Mol. Pharm.* **2015,** *12*, 954-965.

488 10. Kontogianni, V. G.; Charisiadis, P.; Margianni, E.; Lamari, F. N.; Gerothanassis, I.
489 P.; Tzakos, A. G. Olive leaf extracts are a natural source of advanced glycation end
490 product inhibitors. *J. Med. Food* **2013,** *16*, 817-822.

491 11. Kontogianni, V. G.; Tomic, G.; Nikolic, I.; Nerantzaki, A. A.; Sayyad, N.; Stosic-
492 Grujicic, S.; Stojanovic, I.; Gerothanassis, I. P.; Tzakos, A. G. Phytochemical profile of
493 Rosmarinus officinalis and Salvia officinalis extracts and correlation to their antioxidant
494 and anti-proliferative activity. *Food Chem* **2013,** *136*, 120-129.

12. Vasilopoulou, C. G.; Kontogianni, V. G.; Linardaki, Z. I.; Iatrou, G.; Lamari, F. N.; Nerantzaki, A. A.; Gerothanassis, I. P.; Tzakos, A. G.; Margarity, M. Phytochemical composition of "mountain tea" from Sideritis clandestina subsp. clandestina and evaluation of its behavioral and oxidant/antioxidant effects on adult mice. *Eur. J. Nutr.* **2013,** *52*, 107-116.

13. Tzakos, A. G.; Kontogianni, V. G.; Tsoumani, M.; Kyriakou, E.; Hwa, J.; Rodrigues, F. A.; Tselepis, A. D. Exploration of the antiplatelet activity profile of betulinic acid on human platelets. *J. Agric. Food Chem.* **2012,** *60*, 6977-6983.

14. Vilahur, G.; Badimon, L. Antiplatelet properties of natural products. *Vascul. Pharmacol.* **2013,** *59*, 67-75.

15. Das, L.; Bhaumik, E.; Raychaudhuri, U.; Chakraborty, R. Role of nutraceuticals in human health. *J. Food Sci. Technol.* **2012,** *49*, 173-183.

16. Fuentes, E.; Forero-Doria, O.; Carrasco, G.; Marican, A.; Santos, L. S.; Alarcon, M.; Palomo, I. Effect of tomato industrial processing on phenolic profile and antiplatelet activity. *Molecules* **2013,** *18*, 11526-11536.

17. Estruch, R.; Ros, E.; Salas-Salvado, J.; Covas, M. I.; Corella, D.; Aros, F.; Gomez-Gracia, E.; Ruiz-Gutierrez, V.; Fiol, M.; Lapetra, J.; Lamuela-Raventos, R. M.; Serra-Majem, L.; Pinto, X.; Basora, J.; Munoz, M. A.; Sorli, J. V.; Martinez, J. A.; Martinez-Gonzalez, M. A. Primary prevention of cardiovascular disease with a Mediterranean diet. *N. Engl. J. Med.* **2013,** *368*, 1279-1290.

515 18. Ostertag, L. M.; O'Kennedy, N.; Horgan, G. W.; Kroon, P. A.; Duthie, G. G.; de
516 Roos, B. In vitro anti-platelet effects of simple plant-derived phenolic compounds are
517 only found at high, non-physiological concentrations. *Mol. Nutr. Food Res.* **2011,** *55*,
518 1624-1636.

519 19. El, S. N.; Karakaya, S. Olive tree (Olea europaea) leaves: potential beneficial
520 effects on human health. *Nutr. Rev.* **2009,** *67*, 632-638.

521 20. Singh, I.; Mok, M.; Christensen, A. M.; Turner, A. H.; Hawley, J. A. The effects
522 of polyphenols in olive leaves on platelet function. *Nutr. Metab. Cardiovasc. Dis.* **2008,**
523 *18*, 127-132.

524 21. Petroni, A.; Blasevich, M.; Salami, M.; Papini, N.; Montedoro, G. F.; Galli, C.
525 Inhibition of platelet aggregation and eicosanoid production by phenolic components of
526 olive oil. *Thromb. Res.* **1995,** *78*, 151-160.

527 22. Karantonis, H. C.; Antonopoulou, S.; Perrea, D. N.; Sokolis, D. P.; Theocharis, S.
528 E.; Kavantzas, N.; Iliopoulos, D. G.; Demopoulos, C. A. In vivo antiatherogenic
529 properties of olive oil and its constituent lipid classes in hyperlipidemic rabbits. *Nutr.*
530 *Metab. Cardiovasc. Dis.* **2006,** *16*, 174-185.

531 23. Duquesnoy, E.; Castola, V.; Casanova, J. Triterpenes in the hexane extract of
532 leaves of Olea europaea L.: analysis using ^{13}C-NMR spectroscopy. *Phytochem. Anal.*
533 **2007,** *18*, 347-353.

534 24. Kontogianni, V. G.; Exarchou, V.; Troganis, A.; Gerothanassis, I. P. Rapid and
535 novel discrimination and quantification of oleanolic and ursolic acids in complex plant

536 extracts using two-dimensional nuclear magnetic resonance spectroscopy-Comparison
537 with HPLC methods. *Anal. Chim. Acta* **2009,** *635*, 188-195.

538 25. Schrödinger Release 2015-2: LigPrep, version 3.4, Schrödinger, LLC, New York,
539 NY, 2015.

540 26. Jorgensen, W. L.; Maxwell, D. S.; Tirado-Rives, J. Development and testing of the
541 OPLS all-atom force field on conformational energetics and properties of organic liquids.
542 *J. Am. Chem. Soc.* **1996,** *118*, 11225-11236.

543 27. Small-Molecule Drug Discovery Suite 2015-2: QikProp, version 4.4, Schrödinger,
544 LLC, New York, NY, 2015.

545 28. Schrödinger Release 2015-2: Canvas, version 2.4, Schrödinger, LLC, New York,
546 NY, 2015.

547 29. Duan, J.; Dixon, S. L.; Lowrie, J. F.; Sherman, W. Analysis and comparison of 2D
548 fingerprints: Insights into database screening performance using eight fingerprint methods.
549 . *J. Molec. Graph. Model.* **2010,** *29*, 157-170.

550 30. Dixon, S. L.; Smondyrev, A. M.; Knoll, E. H.; Rao, S. N.; Shaw, D. E.; Friesner,
551 R. A. PHASE: A new engine for pharmacophore perception, 3D QSAR model
552 development, and 3D database screening: 1. Methodology and preliminary results. *J.*
553 *Comput.-Aided Mol. Des.* **2006,** *20*, 647-671.

554 31. Watts, K. S.; Dalal, P.; Murphy, R. B.; Sherman, W.; Friesner, R. A.; Shelley, J. C.
555 ConfGen: A conformational search method for efficient generation of bioactive
556 conformers. *J. Chem. Inf. Model.* **2010,** *50*, 534-546.

557 32. Zhang, C.; Srinivasan, Y.; Arlow, D. H.; Fung, J. J.; Palmer, D.; Zheng, Y.; Green,
558 H. F.; Pandey, A.; Dror, R. O.; Shaw, D. E.; Weis, W. I.; Coughlin, S. R.; Kobilka, B. K.
559 High-resolution crystal structure of human protease-activated receptor 1. *Nature* **2012,**
560 *492*, 387-392.

561 33. Madhavi Sastry, G.; Adzhigirey, M.; Day, T.; Annabhimoju, R.; Sherman, W.
562 Protein and ligand preparation: Parameters, protocols, and influence on virtual screening
563 enrichments. *J. Comput.-Aided Mol. Des.* **2013,** *27*, 221-234.

564 34. Schrödinger Release 2015-2: Maestro, version 10.2, Schrödinger, LLC, New
565 York, NY, 2015.

566 35. Shivakumar, D.; Williams, J.; Wu, Y.; Damm, W.; Shelley, J.; Sherman, W.
567 Prediction of absolute solvation free energies using molecular dynamics free energy
568 perturbation and the OPLS force field. *J. Chem. Theory Comput.* **2010,** *6*, 1509-1519.

569 36. Ed Rainger, G.; Chimen, M.; Harrison, M. J.; Yates, C. M.; Harrison, P.; Watson,
570 S. P.; Lordkipanidze, M.; Nash, G. B. The role of platelets in the recruitment of
571 leukocytes during vascular disease. *Platelets* **2015,** *26*, 507-520.

572 37. Friesner, R. A.; Murphy, R. B.; Repasky, M. P.; Frye, L. L.; Greenwood, J. R.;
573 Halgren, T. A.; Sanschagrin, P. C.; Mainz, D. T. Extra precision glide: Docking and
574 scoring incorporating a model of hydrophobic enclosure for protein-ligand complexes. *J.*
575 *Med. Chem.* **2006,** *49*, 6177-6196.

576 38. Schrödinger Release 2015-2: Prime, version 4.0, Schrödinger, LLC, New York,
577 NY, 2015.

578 39. Li, J.; Abel, R.; Zhu, K.; Cao, Y.; Zhao, S.; Friesner, R. A. The VSGB 2.0 model:
579 a next generation energy model for high resolution protein structure modeling. *Proteins*
580 **2011,** *79*, 2794-2812.

581 40. Harder, E.; Damm, W.; Maple, J.; Wu, C.; Reboul, M.; Xiang, J. Y.; Wang, L.;
582 Lupyan, D.; Dahlgren, M. K.; Knight, J. L.; Kaus, J. W.; Cerutti, D. S.; Krilov, G.;
583 Jorgensen, W. L.; Abel, R.; Friesner, R. A. OPLS3: A Force Field Providing Broad
584 Coverage of Drug-like Small Molecules and Proteins. *J. Chem. Theory Comput.* **2016,** *12*,
585 281-296.

586 41. Mitsios, J. V.; Tambaki, A. P.; Abatzis, M.; Biris, N.; Sakarellos-Daitsiotis, M.;
587 Sakarellos, C.; Soteriadou, K.; Goudevenos, J.; Elisaf, M.; Tsoukatos, D.; Tsikaris, V.;
588 Tselepis, A. D. Effect of synthetic peptides corresponding to residues 313-332 of the
589 alphaIIb subunit on platelet activation and fibrinogen binding to alphaIIbbeta3. *Eur. J.*
590 *Biochem.* **2004,** *271*, 855-862.

591 42. Kouki, A.; Mitsios, J. V.; Sakarellos-Daitsiotis, M.; Sakarellos, C.; Tselepis, A. D.;
592 Tsikaris, V.; Tsoukatos, D. C. Highly constrained cyclic (S,S) -CXaaC- peptides as
593 inhibitors of fibrinogen binding to platelets. *J. Thromb. Haemost.* **2005,** *3*, 2324-2330.

594 43. Claude, B.; Morin, P.; Lafosse, M.; Andre, P. Evaluation of apparent formation
595 constants of pentacyclic triterpene acids complexes with derivatized beta- and gamma-
596 cyclodextrins by reversed phase liquid chromatography. *J. Chromatogr. A* **2004,** *1049*, 37-
597 42.

598 44. Lee, J. J.; Jin, Y. R.; Lim, Y.; Yu, J. Y.; Kim, T. J.; Yoo, H. S.; Shin, H. S.; Yun,
599 Y. P. Oleanolic acid, a pentacyclic triterpenoid, induces rabbit platelet aggregation

600 through a phospholipase C-calcium dependent signaling pathway. *Arch. Pharmacal Res.*
601 **2007,** *30*, 210-214.

602 45. Kim, M.; Han, C.-H.; Lee, M.-Y. Enhancement of platelet aggregation by ursolic
603 Acid and oleanolic Acid. *Biomol Ther (Seoul).* **2014,** *22*, 254-259.

604 46. Babalola, I. T.; Shode, F. O.; Adelakun, E. A.; Opoku, A. R.; Mosa, R. A. Platelet-
605 Aggregation Inhibitory Activity of Oleanolic Acid, Ursolic Acid, Betulinic Acid, and
606 Maslinic Acid. *J. Pharmacogn. Phytochem.* **2013,** *1*, 54-60.

607 47. Smyth, S. S.; McEver, R. P.; Weyrich, A. S.; Morrell, C. N.; Hoffman, M. R.;
608 Arepally, G. M.; French, P. A.; Dauerman, H. L.; Becker, R. C. Platelet functions beyond
609 hemostasis. *J. Thromb. Haemost.* **2009,** *7*, 1759-1766.

610 48. Rosado, J. A.; Meijer, E. M.; Hamulyak, K.; Novakova, I.; Heemskerk, J. W.;
611 Sage, S. O. Fibrinogen binding to the integrin alpha(IIb)beta(3) modulates store-mediated
612 calcium entry in human platelets. *Blood* **2001,** *97*, 2648-2656.

613 49. Li, Z.; Delaney, M. K.; O'Brien, K. A.; Du, X. Signaling during platelet adhesion
614 and activation. *Arterioscler. Thromb. Vasc. Biol.* **2010,** *30*, 2341-2349.

615 50. Davey, M. G.; Luscher, E. F. Actions of thrombin and other coagulant and
616 proteolytic enzymes on blood platelets. *Nature* **1967,** *216*, 857-858.

617 51. Hamm, C. W.; Bassand, J. P.; Agewall, S.; Bax, J.; Boersma, E.; Bueno, H.; Caso,
618 P.; Dudek, D.; Gielen, S.; Huber, K.; Ohman, M.; Petrie, M. C.; Sonntag, F.; Uva, M. S.;
619 Storey, R. F.; Wijns, W.; Zahger, D. ESC Guidelines for the management of acute
620 coronary syndromes in patients presenting without persistent ST-segment elevation: The

621 Task Force for the management of acute coronary syndromes (ACS) in patients presenting
622 without persistent ST-segment elevation of the European Society of Cardiology (ESC).
623 *Eur. Heart J.* **2011,** *32*, 2999-3054.

624 52. Amsterdam, E. A.; Wenger, N. K.; Brindis, R. G.; Casey, D. E., Jr.; Ganiats, T. G.;
625 Holmes, D. R., Jr.; Jaffe, A. S.; Jneid, H.; Kelly, R. F.; Kontos, M. C.; Levine, G. N.;
626 Liebson, P. R.; Mukherjee, D.; Peterson, E. D.; Sabatine, M. S.; Smalling, R. W.; Zieman,
627 S. J. 2014 AHA/ACC Guideline for the management of patients with non-ST-Elevation
628 acute coronary syndromes: a report of the American College of Cardiology/American
629 heart association task force on practice guidelines. *J Am Coll Cardiol* **2014,** *64*, e139-228.

630 53. Diehl, P.; Bode, C.; Duerschmied, D. Clinical potential of vorapaxar in
631 cardiovascular risk reduction in patients with atherosclerosis. *Ther. Clin. Risk Manag.*
632 **2015,** *11*, 1133-1138.

633

FIGURE CAPTIONS

Figure 1. (A) 500 MHz ^{1}H-^{13}C HSQC spectrum of the hexane olive leaf extract (40 mg/ ml) (ns= 2, experimental time: 14 min); **(B)** the corresponding ^{1}H-^{13}C HMBC spectrum (ns= 64, mixing time 50 ms, experimental time: 4 h & 16 min).

Figure 2. (A)HPLC/DAD chromatogram (210 nm) of the hexane olive leaf extract; the peaks of oleanolic acid (OA), uvaol(U) and erythrodiol (E) are indicated; **(B)** Dose-response curves for total leaf extract demonstrating the inhibition of platelet aggregation induced by TRAP.

Figure 3. Effect of hexane olive leaf extract and its triterpenoids, erythrodiol, uvaol, oleanolic acid on platelet aggregation at patients with ACS treated with aspirin and ticagrelor.

**p<0.05 in comparison with ADP-induced aggregation in aspirin and ticagrelor, #p<0.05 in comparison with TRAP-induced aggregation in aspirin and ticagrelor.*

Figure 4. (A) Principal components analysis of 11 antithrombotic drugs and the three natural products. The three compounds and atopaxar with vorapaxar (red dots) cluster very closely in the same region (blue). (B) Pharmacophore alignments of: 1. atopaxar (red) with oleanolic acid (gray), 2. atopaxar (red) with uvaol (gray), 3. vorapaxar (blue) with oleanolic acid (gray) and 4. vorapaxar (blue) with uvaol (gray). The three green spheres (H5, H12, H16) represent the common hydrophobic features while the red one represents the H-bond acceptor. (C) Chemical structures of the drugs used in the PCA and their mechanism of action.

Figure 5. Predicted binding poses with best Induced Fit Score of A) oleanolic acid, B) uvaol, C) erythrodiol and D) the crystal structure of vorapaxar in PAR1.

Table 1. Effect of the Hexane Extract of Olive Leaves and its Main Triterpenoids (Erythrodiol,Uvaol, Oleanolic Acid) on Platelet Activation Induced by ADP and TRAP in PRP of Healthy Volunteers.

		Inhibition , %					
		Platelet aggregation		PAC-1 binding		P-selectin expression	
Natural product	Concentration	ADP	TRAP	ADP	TRAP	ADP	TRAP
Total leaf extract	640 µg/ml	32.0 ± 3.0	40.0 ±7.5	67.5±8.0	65.5±5.0	12.0 ± 6.0	49.6±8.0
Erythrodiol	410 µM	42.0 ± 3.0	9.0±2.0	22.0±8.0	8.0±3.0	31.0 ±5.0	9.5±6.4
Uvaol	300 µM	3.0±2.0	98.5 ± 1.5	5.5±6.5	85.5±5.2	8.5±4.0	54.8±3.1
Oleanolic acid	210 µM	3.0±2.5	56.7 ± 3.9	6.0±4.0	92.0 ± 3.0	9.5±4.5	75.8 ±3.4

Table shows the concentration of each natural product that induces the maximum inhibitory effect in each platelet parameters studied.

Values represent the mean ± SD from at least three experiments.

ADP: Adenosine diphosphate, PRP: Platelet-rich plasma, TRAP: Thrombin Receptor Activator Peptide.

Table 2: Prime MM-GBSA Energies for Erythrodiol, Uvaol and Oleanolic Acid Docked in the PAR1 Crystal Structure 3VW7.

	Δ*G*Binding (kcal/mol)	Coulomb[a]	Covalent[b]	Hbond[c]	Lipo[d]	Solv_GB[e]	vdW[f]
Erythrodiol	-24.04	-0.93	0.63	-0.36	-13.67	5.95	-16.01
Uvaol	-37.50	-8.13	-2.69	-0.58	-14.02	9.71	-21.78
Oleanolic Acid	-40.52	-0.27	-4.31	-0.08	-16.89	4.94	-23.91

[a]Coulomb: Coulomb energy; [b]Covalent: Covalent binding energy; [c]vdW: Van der Waals energy; [d]Lipo: Lipophilic energy; [e]Solv_GB: Generalized Born electrostatic solvation energy; [f]Hbond: Hydrogen-bonding energy

634

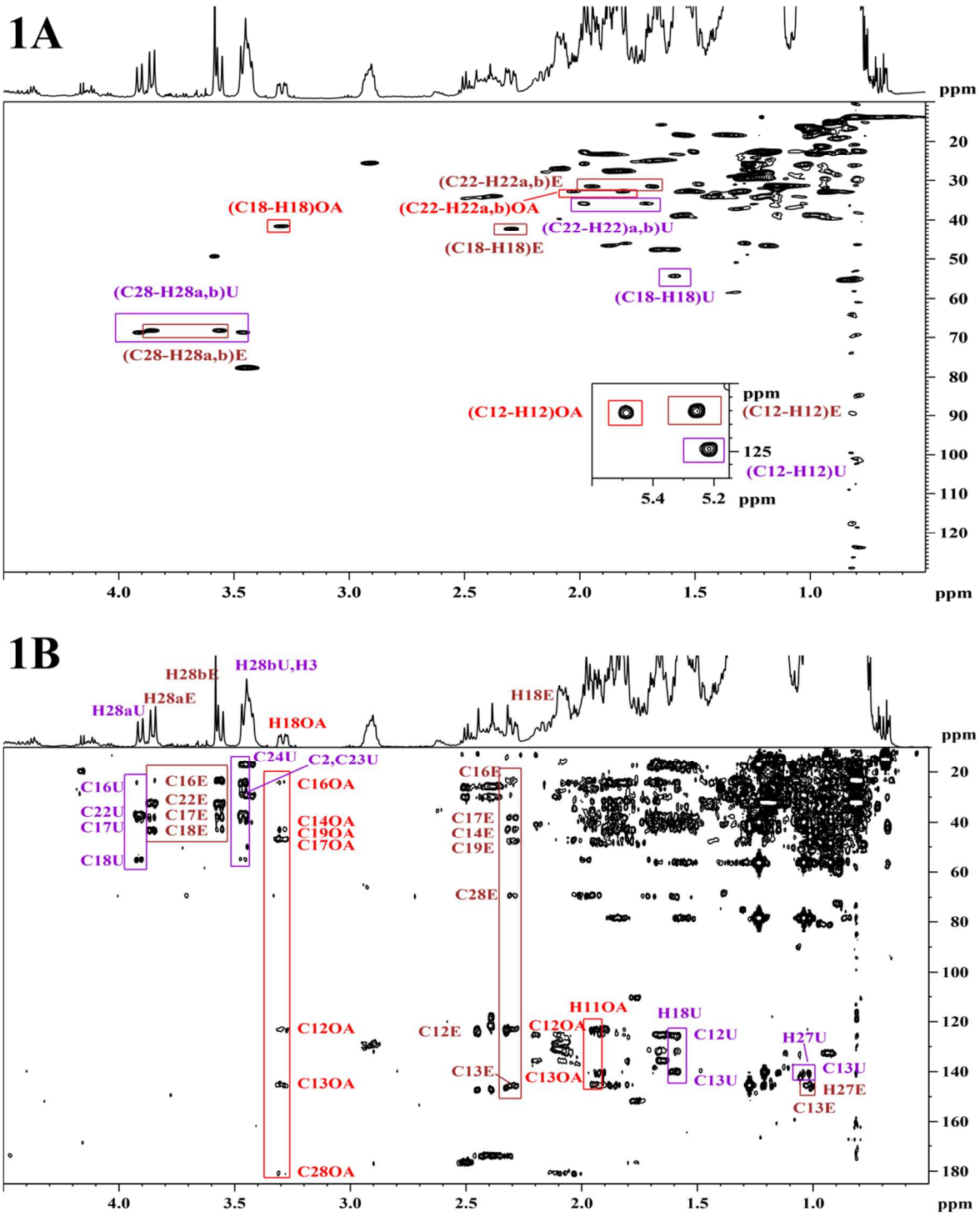
1A
ppm
(C22-H22a,b)E
(C18-H18)OA
(C22-H22a,b)OA
(C22-H22)a,b)U
(C18-H18)E
(C18-H18)U
(C28-H28a,b)U
(C28-H28a,b)E
(C12-H12)OA
ppm
(C12-H12)E
125
(C12-H12)U
5.4
5.2
ppm
4.0
3.5
3.0
2.5
2.0
1.5
1.0
ppm
1B
H28aU
H28aE
H28bE
H28bU,H3
H18OA
H18E
C24U
C2,C23U
C16U
C16E
C22E
C22U
C17E
C17U
C18E
C18U
C16OA
C14OA
C19OA
C17OA
C12OA
C13OA
C28OA
C16E
C17E
C14E
C19E
C28E
C12E
C13E
H11OA
C12OA
C13OA
H18U
C12U
C13U
H27U
C13U
H27E
C13E
ppm
4.0
3.5
3.0
2.5
2.0
1.5
1.0
ppm

Figure 1

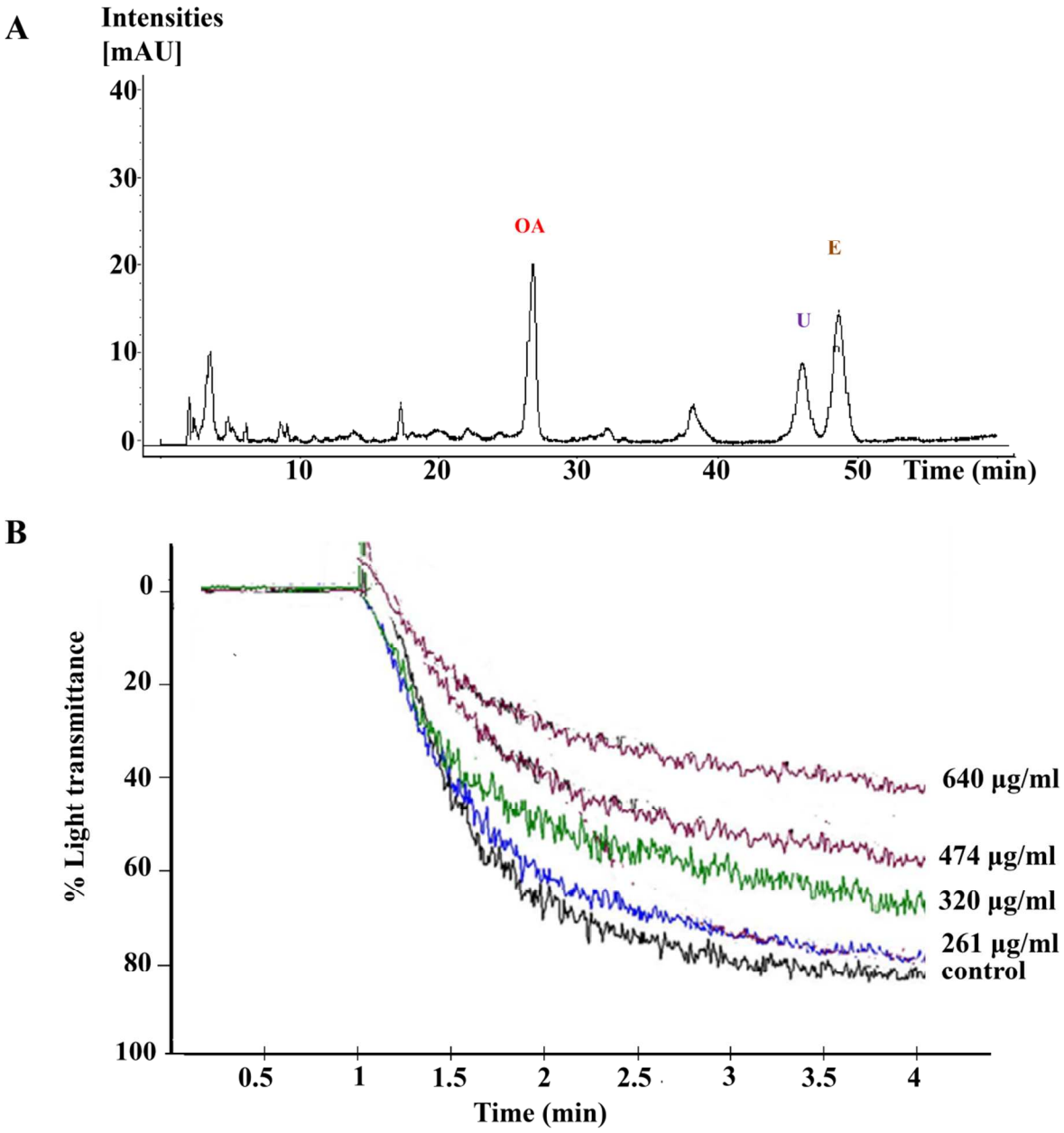
A
Intensities
[mAU]
40
30
20
10
0
OA
E
U
10
20
30
40
50
Time (min)
B
% Light transmittance
0
20
40
60
80
100
640 µg/ml
474 µg/ml
320 µg/ml
261 µg/ml
control
0.5
1
1.5
2
2.5
3
3.5
4
Time (min)

Figure 2

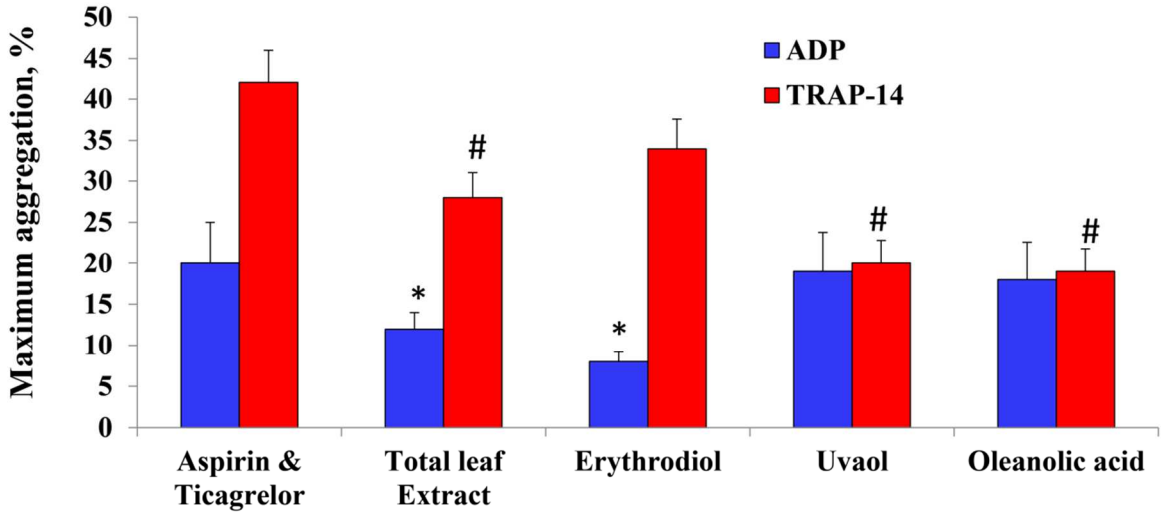
Maximum aggregation, %
50
45
40
35
30
25
20
15
10
5
0
ADP
TRAP-14
*
#
*
#
#
Aspirin & Ticagrelor
Total leaf Extract
Erythrodiol
Uvaol
Oleanolic acid

Figure 3

635

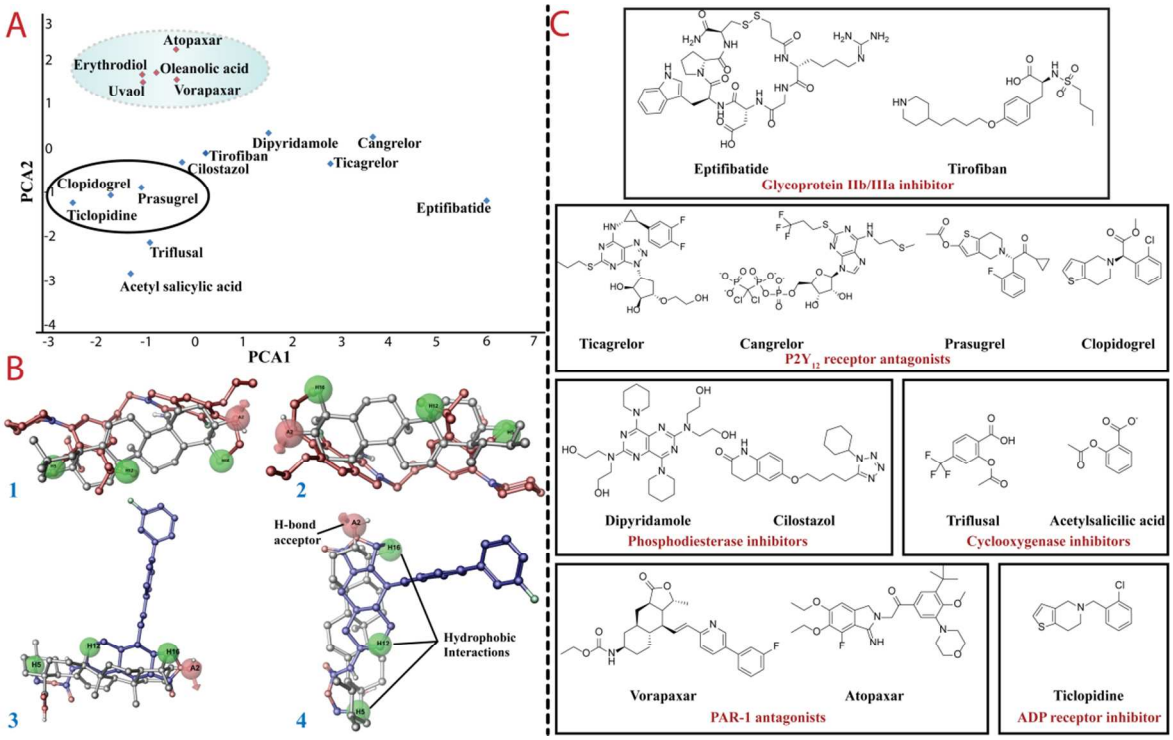
A
Atopaxar
Erythrodiol
Oleanolic acid
Uvaol
Vorapaxar
Dipyridamole
Cangrelor
Tirofiban
Ticagrelor
Cilostazol
Clopidogrel
Prasugrel
Ticlopidine
Eptifibatide
Triflusal
Acetyl salicylic acid
PCA2
PCA1
B
1
2
3
4
H-bond acceptor
Hydrophobic Interactions
C
Eptifibatide
Tirofiban
Glycoprotein IIb/IIIa inhibitor
Ticagrelor
Cangrelor
Prasugrel
Clopidogrel
P2Y12 receptor antagonists
Dipyridamole
Cilostazol
Phosphodiesterase inhibitors
Triflusal
Acetylsalicilic acid
Cyclooxygenase inhibitors
Vorapaxar
Atopaxar
PAR-1 antagonists
Ticlopidine
ADP receptor inhibitor

Figure 4

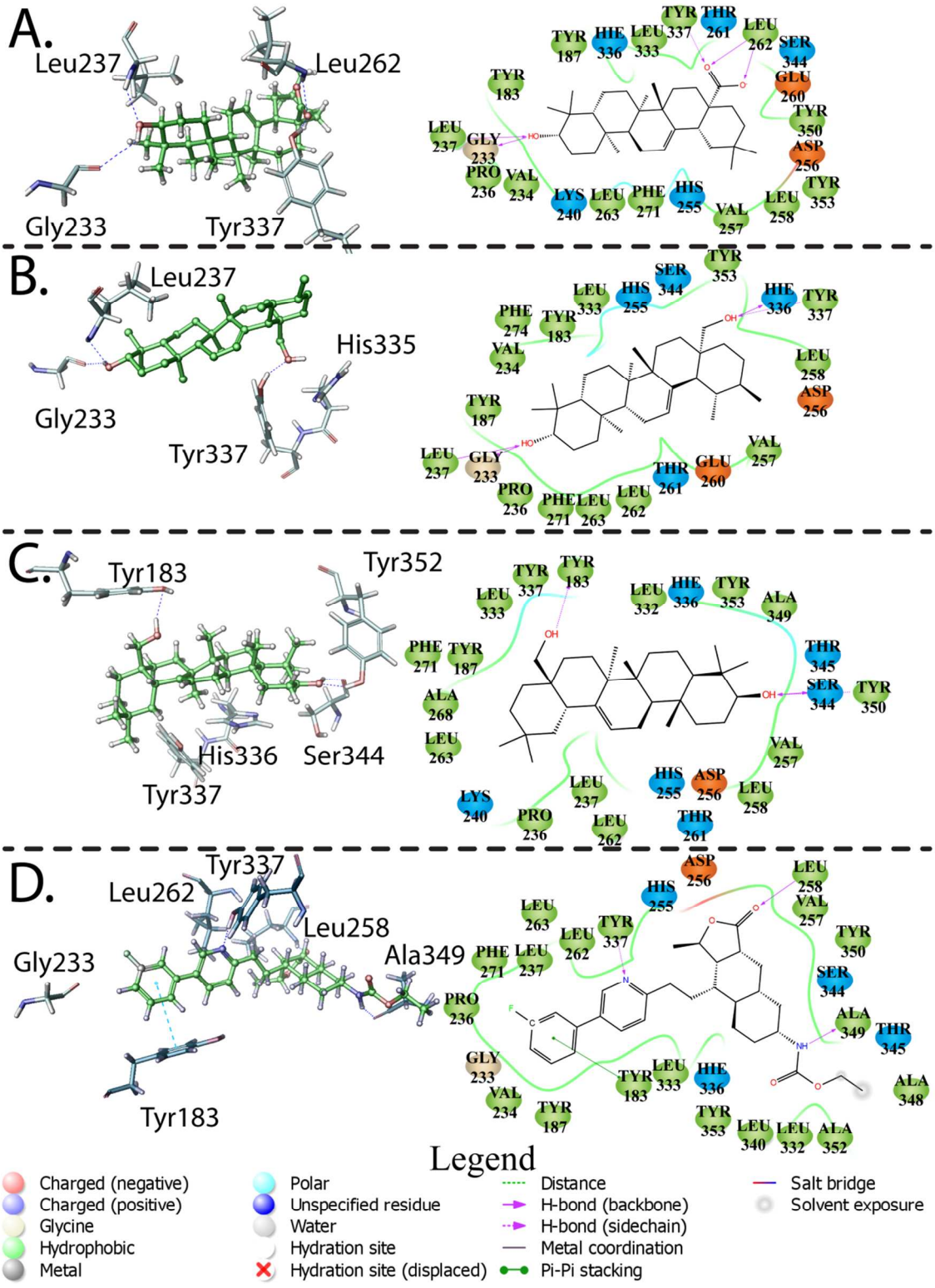
A.
Leu237
Leu262
Gly233
Tyr337
B.
Leu237
His335
Gly233
Tyr337
C.
Tyr183
Tyr352
His336
Ser344
Tyr337
D.
Tyr337
Leu262
Leu258
Ala349
Gly233
Tyr183
Legend
Charged (negative)
Charged (positive)
Glycine
Hydrophobic
Metal
Polar
Unspecified residue
Water
Hydration site
Hydration site (displaced)
Distance
H-bond (backbone)
H-bond (sidechain)
Metal coordination
Pi-Pi stacking
Salt bridge
Solvent exposure

Figure 5

Table of Contents Graphic (TOC)